

Structural Peculiarities Dominate the Turgor Pressure Response of the Marine Alga *Valonia utricularis* upon Osmotic Challenges

M. Heidecker, S. Mimietz, L.H. Wegner, U. Zimmermann

Lehrstuhl für Biotechnologie der Universität Würzburg, Biozentrum, Am Hubland, D-97074 Würzburg, Germany

Received: 15 August 2002/Revised: 1 December 2002

Abstract. The pressure response of (plant) cells to osmotic challenges depends on the reflection coefficient, σ , of osmotically active solutes; it is less than predicted by the van't Hoff equation if $\sigma < 1$. In *Valonia utricularis*, σ is significantly reduced by internal (and, to a lesser extent, by external) unstirred layers, protecting the cytoplasm against vacuolar osmotic fluctuations. As shown by scanning and transmission electron microscopy, diffusion-restricted spaces are formed by innumerable small vacuoles that are interconnected with each other and with the central vacuole. They are embedded in networks of cytoplasmic strands connecting and encircling the organelles. Unstirred layers are also created in the central vacuole by an extensive network of acid mucopolysaccharide filaments (visualized by alcian blue staining). Mucopolysaccharides apparently also affect steady-state turgor by reducing the water activity. When the effective vacuolar osmotic pressure was adjusted to that of the bath by perfusion with an artificial vacuolar sap (AVS), an 'offset turgor pressure' of 17 ± 5 kPa was recorded.

Consistent with the ultrastructural data, σ values less than unity were calculated from the pressure response upon vacuolar addition of KCl or sucrose by perfusion ($\sigma_{iKCl} = 0.63 \pm 0.13$; $\sigma_{isuc} = 0.58 \pm 0.17$). Dilution of AVS yielded slightly higher σ_{iKCl} values (0.73 ± 0.35).

External addition to the artificial sea water (ASW) indicated that $\sigma_e > \sigma_i$ for these osmotica. However, even in this case, σ_{esuc} (0.86 ± 0.09) and σ_{ePEG} (0.58 ± 0.08) were significantly less than σ_{eNaCl} (0.94 ± 0.05) and σ_{eKCl} (0.91 ± 0.13), presumably due to unstirred layers within the 4 μm thick cell wall. Consistent with the low σ values, a partial replacement of NaCl by osmotically equivalent

amounts of sucrose (ASW_{suc}), PEG and dextran, respectively, as well as replacement of Cl^- by the large anion MES^- induced an 'anomalous' hypotonic turgor pressure response followed by the usual backregulation of pressure. After a 2-day preincubation in ASW_{suc}, significantly lower σ_e values were obtained both hyperosmotically ($\sigma_{eNaCl} = 0.78 \pm 0.14$; $\sigma_{esuc} = 0.72 \pm 0.15$) and hypototically ($\sigma_{eNaCl} = 0.70 \pm 0.17$; $\sigma_{esuc} = 0.63 \pm 0.09$), probably due to long-term effects on membrane structure to be elucidated yet.

The freshwater alga *Chara corallina* lacked these apparently closely related structural and biophysical features of *Valonia*.

Key words: Pressure probe — Tonoplast — Plasmalemma — Folded membrane — Cell wall — Reflection coefficient

Introduction

Fluxes across biological membranes can be coupled to nonconjugated as well as conjugated forces. Well-known examples are the phenomena of swelling and shrinking of wall-less cells and of turgor pressure regulation in response to external osmotic pressure changes in walled cells (Dainty & Ginzburg, 1963; Zimmermann, 1978, 1989; Gutknecht, Hastings & Bisson, 1978; Tomos & Wyn Jones, 1988; Chamberlin & Strange, 1989; Kirst, 1990; Chan & Nelson, 1992; Kirk, 1997; Shepherd, Beilby & Heslop, 1999; Stent et al., 2000; Findlay, 2001).

The thermodynamics of irreversible processes shows (Kedem & Katchalsky, 1958; Katchalsky & Curran, 1965; House, 1974; Sauer, 1978) that the full van't Hoff osmotic pressure ($\pi = cRT$) is only developed for ideal semipermeable membranes. For solute-permeable membranes the osmotic (or hydrostatic) pressure changes are usually less than predicted

by the van't Hoff equation. The ratio of the apparent osmotic (or hydrostatic) pressure response to the osmotic pressure change calculated from the concentration of the solute is defined as the reflection coefficient, σ (at volume flow equilibrium). Alternatively, σ can be defined by $\sigma = -L_{pd}/L_p$ where L_{pd} is the osmotic (ultrafiltration) coupling coefficient and L_p the hydraulic conductivity of the membrane barrier (Dainty & Ginzburg, 1963; Zimmermann & Steudle, 1978). For single cells, the magnitude of σ normally ranges between 0 and 1 depending on the nature of the solute and the characteristics of the membrane.

For electrolytes the reflection coefficient can attain negative values, e.g., in mosaic membranes made up of parallel and oppositely charged elements (Kedem & Katchalsky, 1961, 1963). Occurrence of negative σ values means that the membrane exhibits 'anomalous' osmosis where volume flow occurs in the opposite direction to that indicated by the apparent osmotic pressure gradient.

Reflection coefficients can, in principle, be determined by the measurement of osmotically induced changes in cell volume (Verkman, 2000; Curry, Shachar-Hill & Hill, 2001) or hydrostatic (turgor) pressure (Zimmermann & Steudle, 1974; Zimmermann, 1978). Plant cells, which are stabilized by a cell wall, generally exhibit regulation of their turgor pressure in response to osmotic stress because of the high volumetric elastic modulus of the wall (for exception, see Zimmermann & Hüsken, 1979). Changes in turgor pressure can be monitored very precisely by using the pressure probe technique (Zimmermann, Råde & Steudle, 1969; Zimmermann & Steudle, 1978; Zimmermann, 1978). Reflection coefficients can be calculated from pressure relaxation curves, as detailed elsewhere (Zimmermann & Steudle, 1970).

However, in practice, problems can arise from unstirred layer effects (and related effects such as concentration polarization, sweep-away and transport-number effects; see e.g., Dainty & Ginzburg, 1963; Barry & Hope, 1969; House, 1974; Barry & Diamond, 1984; Verkman & Dix, 1984; Ling, 1987; Verkman, 2000). Unstirred layers are regions of poorly mixed solution in which solute transport occurs by diffusion alone. The presence of unstirred layers can lead to an apparent underestimation of parameters (including reflection coefficients) because of the discrepancy between the nominal value of the concentration gradient between the bathing solution and the vacuole and the actual concentration gradient across the membrane (Pohl, Saporov & Antonenko, 1997).

In this communication we demonstrate that unstirred layers can lead to a dramatic underestimation of the reflection coefficients for non-electrolytes, even for macromolecules, such as PEG, widely used as an osmolyte by plant physiologists. Under some circumstances this can lead to 'anomalous' turgor

pressure responses under isosmotic conditions, as shown here for the giant marine alga *Valonia utricularis*. Studies have shown (Zimmermann, Steudle & Lelkes, 1976; Zimmermann & Steudle, 1978; Guggino & Gutknecht, 1982; Heidecker et al., 2003) that this species tolerates a relatively large range of salinities by appropriate adjustment of turgor pressure. Hyperosmotic challenges are managed by formation of ATP- and pressure-dependent (colocalized) K^+ and Cl^- transporters within the plasmalemma, resulting in KCl and water influx until the original turgor pressure is restored. Conversely, hyposmotic challenges are overcome by increased passive KCl efflux due to an increase of the volumetric elastic modulus of the cell wall with pressure (Zimmermann & Steudle, 1978). Electrophysiological studies have given evidence (Wang et al., 1997; Ryser et al., 1999) that the tonoplast must be multi-folded, leading to a sponge-like organization of the 5 μm thick cytoplasmic layer situated between the large central vacuole (occupying more than 95% of the cell volume) and the cell wall.

Scanning and transmission electron microscopy of cells (fixed in the turgescence state) performed in the present study confirm these structural features of the vacuole. The vacuolar infoldings are regions ideal for the development of huge unstirred layers. Staining with alcian blue additionally shows an extended network of acid mucopolysaccharides within the central vacuole, which may also contribute—among other things—to the formation of unstirred regions in this compartment. Consistent with these structural features, it was found that the values of the vacuolar reflection coefficients of KCl, sucrose and PEG (derived from perfusion of the vacuole with solutions of appropriate osmotic pressure) were significantly less than the external reflection coefficients of these osmolytes as well as of other sugars and macromolecules. The external reflection coefficients were generally also smaller than unity, arising from unstirred layer effects in the 4 μm thick cell wall and presumably from some specific interactions of the osmolytes with the wall, plasmalemma and/or the spongy architecture of the cytoplasm, as suggested by analogous measurements on the pond water alga *Chara corallina*.

Extended internal and external unstirred regions, as detected here for *V. utricularis* by using different methodological approaches, can obviously protect the cytoplasm of this species against fluctuations of the osmotic pressure in the vacuole occurring under natural conditions because equilibration can only be achieved by slow diffusion processes. Dramatic membrane infoldings are also seen in cells of higher plants, e.g., plasmalemma infoldings in transfer cells due to cell wall ingrowths (Pate & Gunning, 1972; Läuchli et al., 1976). Furthermore, extracellular mucilage was found in other algae (e.g., Shepherd & Beilby, 1999 and literature quoted there) as well as in

the xylem and cells of tall trees rooting in high-salinity water (Zimmermann et al., 1994, 2002). Thus, unstirred layer effects may have a much more subtle ecological significance for the water balance of higher plants than hitherto assumed.

Materials and Methods

PLANT MATERIAL

Valonia utricularis

Cells of *V. utricularis* (*Cladophorales*, *Chlorophyceae*) were collected at Ischia, in the gulf of Naples, Italy, and kept in 40-liter tanks of Mediterranean sea water (MSW, osmolality $\pi_e = 1127$ mosmol kg^{-1} , pH 8.1) under a 12 h light/dark regime (2×36 W Fluora lamps, Osram, Munich, Germany) at 16°C. Geometrically even cells with volumes between 50 and 160 μl were used throughout the experiments. The cells were clamped in a small PerspexTM chamber perfused with artificial sea water (ASW) containing in mM) 545 NaCl, 12 KCl, 11 CaCl_2 and 10 MgCl_2 (Merck, Darmstadt, Germany). The pH was adjusted to 8.1 by addition of 10 mM HEPES/NaOH (Sigma, Deisndorf, Germany). The osmotic pressure of the buffered ASW was determined cryoscopically to be 1127 mosmol kg^{-1} by using the Osmomat 030 (Gonotec GmbH, Berlin, Germany). The conductivity was measured to be 51 mS cm^{-1} by using a conductometer (Knick, Berlin, Germany). The experiments were performed at about 20°C.

Chara corallina

C. corallina was obtained from U. Hansen, Kiel, and cultivated in 40-liter tanks filled with distilled water at room temperature under a day-light regime. The bottom of the tanks was covered with a 5 cm thick layer of soil. For experiments, *Chara* cells were bathed in artificial pond water (APW) containing 1 mM NaCl, 0.1 mM KCl, 0.1 mM CaCl_2 , 0.1 mM MgCl_2 and 1 mM HEPES (pH 5.5, osmolality 8 mosmol kg^{-1}).

TURGOR PRESSURE RELAXATIONS

The turgor pressure of *C. corallina* was recorded with the oil-filled pressure probe at about 20°C, as described in detail elsewhere (Zimmermann et al., 1969; Zimmermann & Steudle, 1974). The effect of sucrose on turgor pressure was determined by lowering first the initial turgor pressure from about 0.5 MPa to about 0.4 to 0.1 MPa by exchange of APW with APW to which 40 to 160 mosmol kg^{-1} NaCl had been added. Then, after establishment of a new pressure equilibrium, NaCl was replaced isoosmotically by sucrose and the pressure response was recorded.

The oil-filled cell pressure probe was also used for measurements on cells of *V. utricularis*. However, in most experiments, the pressure-controlled perfusion assembly with integrated potential-measuring setup was used (for details and a schematic representation of the setup, see Wang et al., 1997). Briefly, the perfusion setup allows independent control of perfusion flow rate and turgor pressure and allows the exchange of perfusion solutions without a pressure shock. It is also possible to adjust any pressure using a regulator valve and pressure chamber without changing the osmotic pressure of the bath. Experiments with the oil-filled pressure probe and the perfusion assembly yielded similar pressure responses on osmotic stress — at least within the limits of accuracy. Turgor pressure relaxations were induced by addition of low- or

high-molecular-weight non-electrolytes and electrolytes to ASW (and AVS, see below) or by isosmotic substitution of NaCl in the ASW. Isosmotic replacement of part of the NaCl in the ASW by non-electrolytes or electrolytes is denoted by subscripts (e.g., ASW_{suc,160} means that 160 mosmol kg^{-1} NaCl was replaced by 160 mosmol kg^{-1} sucrose). If not otherwise stated, the osmolality of the modified ASW media was adjusted to about 1127 mosmol kg^{-1} .

For the study of the effect on turgor pressure of sucrose added to the vacuolar side, the algae were first perfused (at constant pressure) with artificial vacuolar sap (AVS) containing (in mM) 210 NaCl, 3 CaCl_2 , 3 MgCl_2 , 3 phosphate buffer and 420 KCl (pH 6.3, 1210 mosmol kg^{-1} , perfusion rate 10 $\mu\text{l min}^{-1}$). After about 60 min, perfusion was stopped. Previous experiments had shown (Wang et al., 1997) that this perfusion time was sufficient to completely exchange the vacuolar sap (50 to 160 μl) by AVS. Then, the perfused cell was subjected to a perfusion regime outlined below, in order to test the effect of addition of sucrose or of isosmotic replacement of KCl by sucrose.

CALCULATION OF VACUOLAR AND EXTERNAL REFLECTION COEFFICIENTS

The relaxation measurements allow calculation of the external and internal reflection coefficients of solutes, σ_e and σ_i , provided that the volumetric elastic modulus of the cell wall, ε , and the initial vacuolar osmotic pressure, π_{i0} , are known. As shown by Zimmermann and Steudle (1974), the turgor pressure difference, ΔP , between the initial and final pressure ($\Delta P = P_0 - P_f$) is given by Eq. 1:

$$\Delta P = \frac{\varepsilon \sigma \Delta \pi_{e,i}}{\varepsilon + \pi_{i0}} \quad (1)$$

where σ is the external or internal reflection coefficient (denoted below as σ_e and σ_i) and $\Delta \pi$, the corresponding change in osmotic pressure upon vacuolar or external addition of the osmotically active solute, ε is given by Eq. 2 (Philip, 1958):

$$\varepsilon = \Delta P_1 \frac{V_0}{\Delta V_1} \quad (2)$$

The volumetric elastic modulus can easily be determined by injection of volume increments, ΔV_i , of increasing amplitude into the cell and by simultaneous measurement of the corresponding changes in turgor pressure, ΔP_i (for experimental details, see Zimmermann & Steudle, 1978). The initial volume of the cell, V_0 , was determined microscopically and the vacuolar osmotic pressure, π_{i0} , for calculation of σ_e was estimated from $\pi_{i0} = P_0 + \pi_e$.

It has to be noted that the derivation of Eq. 1 is based on the assumption that the reflection coefficients of the vacuolar ions can be set to unity. Even though this does not hold true for *V. utricularis* (see below), the error in the calculation of σ_e is negligible because ε of marine algae is always much larger than π_{i0} .

The vacuolar reflection coefficients σ_i can also be calculated from Eq. 3 (Zimmermann & Steudle, 1974):

$$\sigma_i = \frac{P_0 + \sigma_e \pi_e}{\pi_i} \quad (3)$$

i.e., by measuring the equilibrium turgor pressure, P_0 , and the osmolality, π_i , cryoscopically in 50 μl of the vacuolar sap extracted afterwards with a micropipette. This has the advantage that the measurement of ε in an independent experiment is not required.

ELECTRON MICROSCOPY

Optimal contrast of membrane structures was obtained when a fixation solution was used consisting of ASW that contained additionally 2% glutaraldehyde, 0.1 M sodium cacodylate and 2%

osmium tetroxide (25% glutaraldehyde stock solution purchased from Merck, Darmstadt, Germany; sodium cacodylate and osmium tetroxide from Roth, Karlsruhe, Germany; final pH of the fixation solution: 8.1) for 2 h at room temperature. Alternatively, some cells were instead exposed to an osmium-free fixation solution (0.1 M sodium cacodylate and 2.5% glutaraldehyde dissolved in ASW). After washing with ASW containing 0.1 M sodium cacodylate, all cells were post-fixed at 47°C for 4 h in a solution made up of ASW with 0.1 M sodium cacodylate and 2% osmium tetroxide (see Zhang & Robinson, 1986). The osmolality of all solutions was adjusted to about 1127 mosmol kg⁻¹, corresponding to the osmolality of the ASW.

During fixation in osmium-free fixation solution the algae remained turgid as revealed by monitoring their turgor pressure via an inserted cell turgor pressure probe (Zimmermann, 1978). Fixed cells were dehydrated in a graded ethanol series and then embedded in Epoxid resin (Serva, Heidelberg, Germany). Ultrathin sections were made with an ultramicrotome (MT-7000, Ultra, RMC, Tucson, AZ). The sections were stained with uranyl acetate and lead citrate (Merck) and then examined on a Zeiss EM 900 and an EM 10 transmission electron microscope (LEO, Oberkochen).

Perfused cells were prepared for transmission electron microscopy using the perfusion assembly to add fixatives both from the external and the vacuolar side. For vacuolar fixation, a fixation solution was used based on artificial vacuolar sap containing 2.5% glutaraldehyde and 0.05 M sodium cacodylate to which 1% tannic acid (Roth) was added. The osmolality and the pH were adjusted to about 1200 mosmol kg⁻¹ and 6.3, respectively.

For scanning electron microscopy the algae were immersed in fixation solution and cut into several pieces. The algae were fixed by using the protocol described above for transmission electron microscopy or incubated in an ASW-based fixation solution containing 6.25% glutaraldehyde for 24 h at 4°C. The cell pieces were dehydrated in a graded acetone series, washed with liquid CO₂ and then critical-point dried (CPD 030, Balzers, Liechtenstein). The dry pieces were mounted on a specimen holder, coated with gold-palladium (SCD 005, Balzers, Liechtenstein) and observed with a scanning electron microscope (Zeiss DSM 962, LEO) at 15 kV.

STAINING OF MUCOPOLYSACCHARIDES WITH ALCIAN BLUE

The presence of acid mucopolysaccharides in the vacuole was demonstrated by perfusing the alga with an AVS solution that was adjusted to pH 2.5 and in which alcian blue (Sigma, Deisenhofen) was dissolved at a concentration of about 0.05%. At this pH, staining is specific for acid mucopolysaccharides (McCully, 1970). In other experiments, the pH of the perfusate was adjusted to the usual value of 6.3. Cells were perfused for at least 1 h at a low rate (2 µl/min) to minimize damages to the filamentous network in the vacuole. Subsequently, alcian blue was washed away with dye-free AVS medium at the same pH.

Results

STRUCTURAL FEATURES OF THE TONOPLAST AND THE CYTOPLASM

As mentioned above, the multi-folded structure of the tonoplast of *Valonia utricularis* (as well as of *Ventricaria ventricosa*) is accompanied by an unusually high area-specific capacitance of $6.2 \cdot 10^{-2} \text{ F m}^{-2}$ for *V. utricularis* (Wang et al., 1997) and of $7.1 \cdot 10^{-2} \text{ F m}^{-2}$

for *V. ventricosa* (Ryser et al., 1999). Scanning electron microscopy (Fig. 1a) in combination with transmission electron microscopy¹ (Fig. 1b) provided further evidence that the peripherally localized vacuolar spaces together with the central vacuole apparently form a continuum. The scanning electron micrograph (Fig. 1a), showing a view onto the cytoplasm from the side of the central vacuole, demonstrates that chloroplasts and nuclei are interconnected by numerous thin cytoplasm strands that surround or sometimes transverse intervening vacuolar spaces, leading to a spongy appearance of the cytoplasm. The variable size of the peripherally localized vacuolar spaces is demonstrated on the electron micrograph of an ultrathin section through the peripheral area of a cell (Fig. 1b). The continuum of the peripherally localized vacuolar spaces with the central vacuole is further supported by vacuolar perfusion experiments with fixation solutions containing 1% tannic acid. Tannic acid was visible as electron-dense particles along the membrane of the central vacuole and also along the boundaries of the vacuolar spaces (*data not shown*). This result can only be explained if the vacuolar spaces are part of the central vacuole. A closer inspection (Fig. 1b) revealed that the cytoplasmic layer that is in direct contact with the cell wall has at some sites a thickness of not more than 40 nm (arrow in Fig. 1b). Nearly all organelles are localized in the several micrometer thick cytoplasmic layer containing vacuolar spaces of variable sizes. There was no evidence for invaginations of the plasmalemma. Even in the thickened wall regions seen sporadically, the plasmalemma was closely aligned along the cell wall. A manuscript showing further details is in preparation.

OFFSET TURGOR PRESSURE IN *VALONIA UTRICULARIS*

Turgor pressure, P , usually assumed a constant value of $0.15 \pm 0.07 \text{ MPa}$ ($n = 200$) 30 min after insertion of the perfusion inlet and outlet capillaries into the vacuole of *V. utricularis*, indicating that leaks were completely resealed. Manipulation of the vacuolar sap by perfusion very frequently resulted in clogging of the tips of the microcapillaries. Perfusion of the vacuole with AVS containing alcian blue at pH 2.5 revealed that a filamentary network of acid mucopolysaccharides existed within the central vacuole (Fig. 2a). This network remained partly intact during perfusion with the dye solution (arrows). A similar network was found when cells were perfused at a pH of 6.3, corresponding to the value under physiological conditions (Fig. 2b). Blue staining of extracted vacuolar sap was also observed at a saturating concentration of alcian blue dissolved in concentrated HCl (pH 1.0).

¹ Independent of the fixation protocol used, very similar organization of the cytoplasmic layer was observed

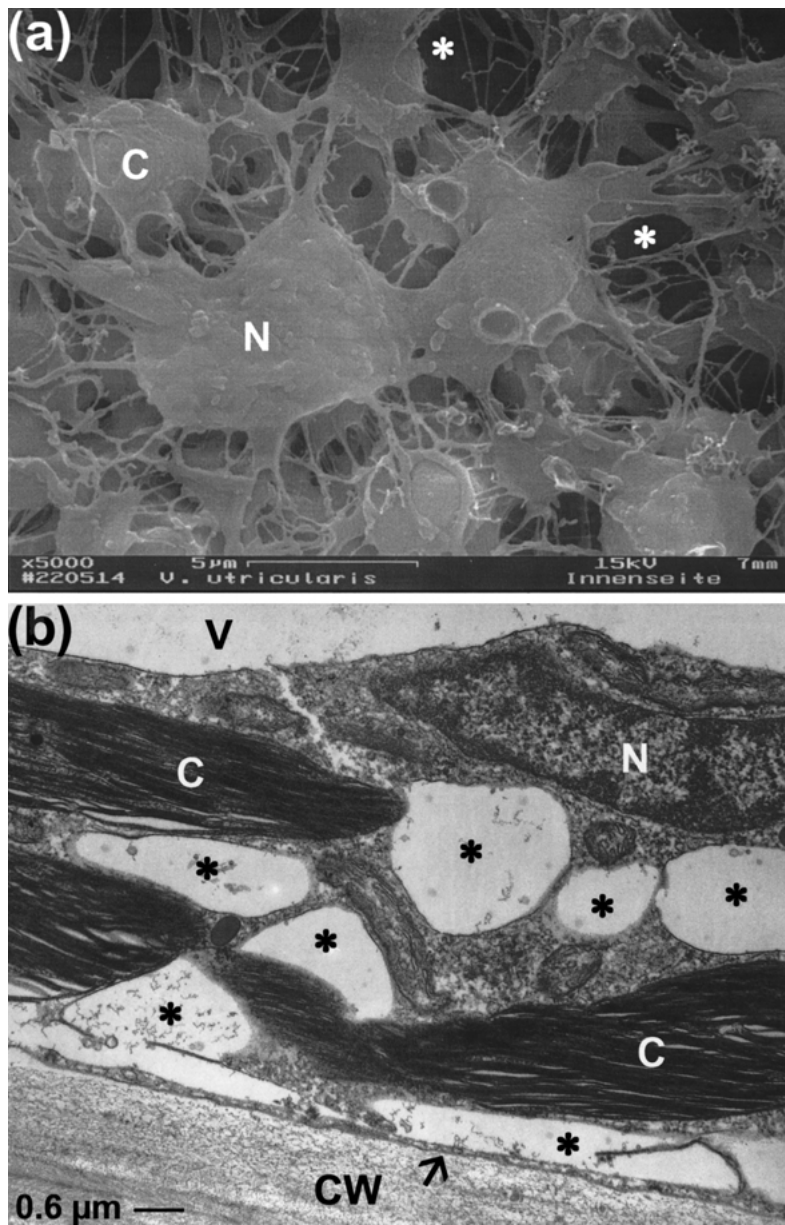


Fig. 1. View onto the cytoplasm from the vacuolar side (a) and cross-sectional view of the cytoplasm (b) of cells of *V. utricularis* by scanning electron microscopy and by transmission electron microscopy, respectively. Cells were fixed in artificial sea water. For fixation details and performance, see text. Abbreviations: C = chloroplasts, CW = cell wall, N = nucleus, V = central vacuole. Asterisks denote vacuolar infoldings. Note the innumerable cytoplasmic strands encircling and interconnecting the chloroplasts and nuclei. The arrow in (b) marks a site at which the tonoplast approaches the plasmalemma (cytoplasmic gap between the membranes about 40 nm).

These mucopolysaccharides apparently contributed to the equilibrium turgor pressure as shown by experiments in which the osmolality of the AVS was matched to the osmolality of ASW by appropriate reduction of the KCl concentration to $\pi_{i0} = 1127$ mosmol kg^{-1} (AVS₁₁₂₇). Even though $\Delta\pi$ was zero and the reflection coefficient of KCl (main component of AVS) in the perfusion solution was somewhat less than NaCl (main component of ASW) in the external medium (see below), the turgor pressure did not vanish. An offset equilibrium pressure of 17 ± 5 kPa ($n = 4$) remained. A typical experiment is shown in Fig. 3. For the accurate determination of the offset turgor pressure it was necessary to lower the turgor pressure stepwise by subjecting the alga five times to a perfusion/pressure release regime

(as indicated by arrows in Fig. 3). This repetition was needed because changes in the volume and thus in the vacuolar osmotic pressure occurred during perfusion in response to significant changes in turgor pressure (see Eq. 2).

As shown in Fig. 3, such changes in π_{i0} were particularly pronounced after the first perfusion step because the turgor pressure decreased by about 0.08 MPa upon release of the clamped pressure. The equilibrium pressure decreased further, but significantly less when the vacuole was perfused a second time by AVS₁₁₂₇ (Fig. 3). A final pressure value was reached after the fourth clamp. Occasionally, a further, but very small decrease in pressure (by a few kPa; see Fig. 3) was recorded after the following perfusion step. Such small pressure changes were

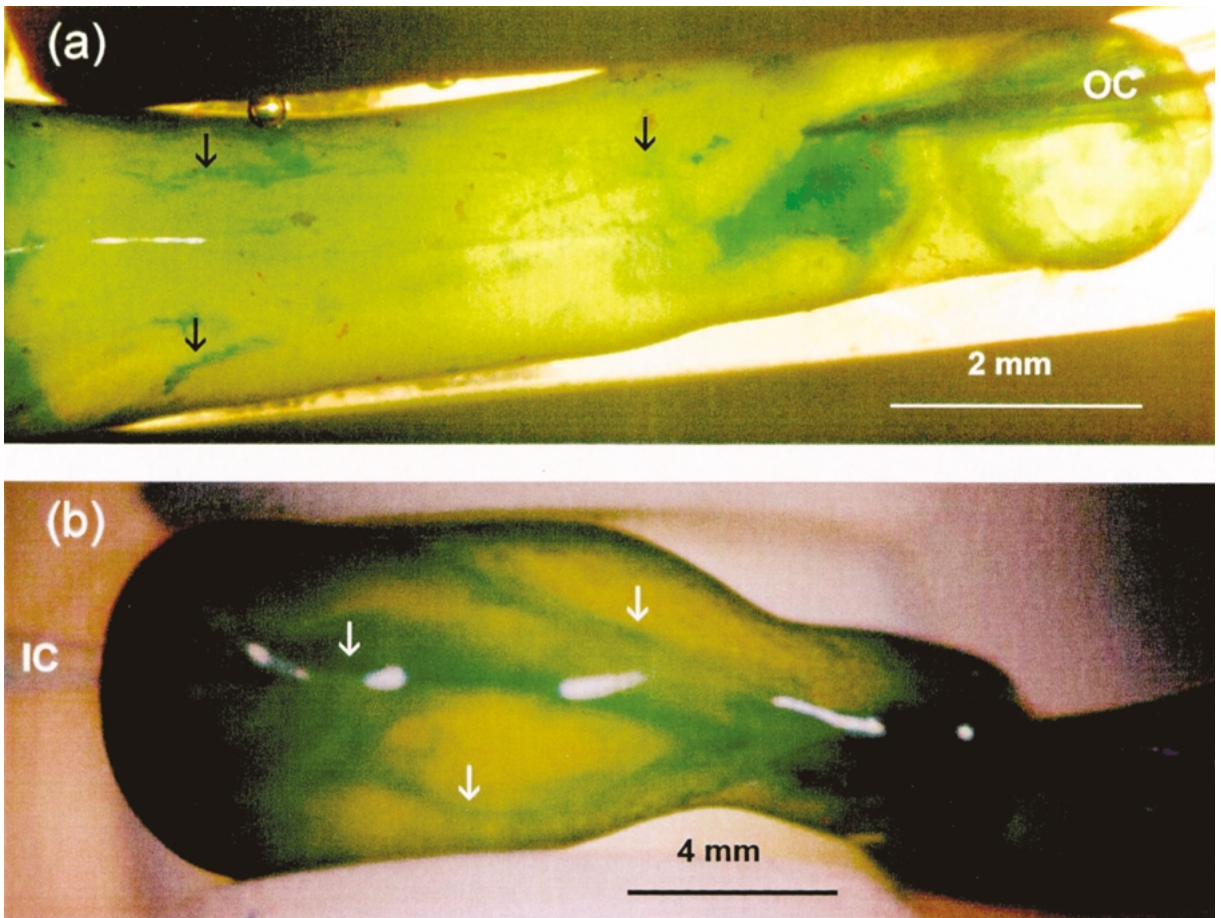


Fig. 2. Filament network of acid mucopolysaccharides in the central vacuole of cells of the marine alga *V. utricularis* (arrows). The algae were incubated in artificial sea water (ASW; pH = 8.1, osmotic pressure $\pi_e = 1127 \text{ mosmol kg}^{-1}$ corresponding to 2.82 MPa) and perfused with artificial vacuolar sap (AVS; $\pi_i = 1210 \text{ mosmol kg}^{-1}$; 'IC' = inlet capillary; 'OC' = outlet capillary) in which alcian blue was dissolved at a saturating concentration of

about 0.05% for at least 1 h. For specific staining of acid mucopolysaccharides, the perfusion medium was adjusted to pH 2.5 (cell shown in *a*). In other experiments, the pH was kept at the usual value of 6.3 (cell shown in *b*). After staining, the vacuole was again perfused with dye-free AVS at the same pH to wash away the residual dye solution.

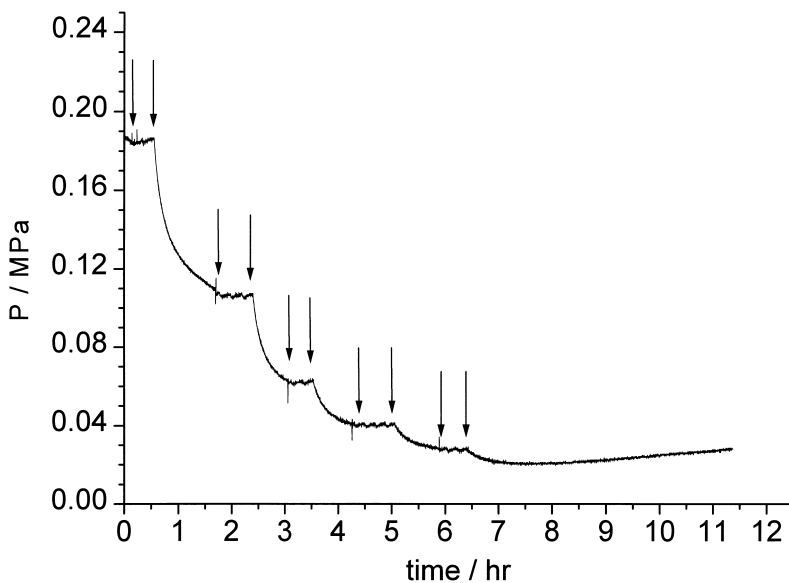


Fig. 3. Determination of the offset turgor pressure apparently arising from the gel-like vacuolar compounds. The alga was successively perfused with AVS while simultaneously clamping the turgor pressure. In contrast to the experiment of Fig. 2, the osmolality of AVS was matched here to the osmolality of ASW by appropriate change of KCl. Between two pressure clamps (indicated by arrows) the pressure was released, resulting in a relaxation of the turgor pressure to a new lower steady-state value. Note that the turgor pressure changes decreased with increasing number of clamps until a final value of 0.03 MPa was reached after the fourth clamp. The very small turgor pressure change observed after the fifth clamp is an artifact (for details, see text).

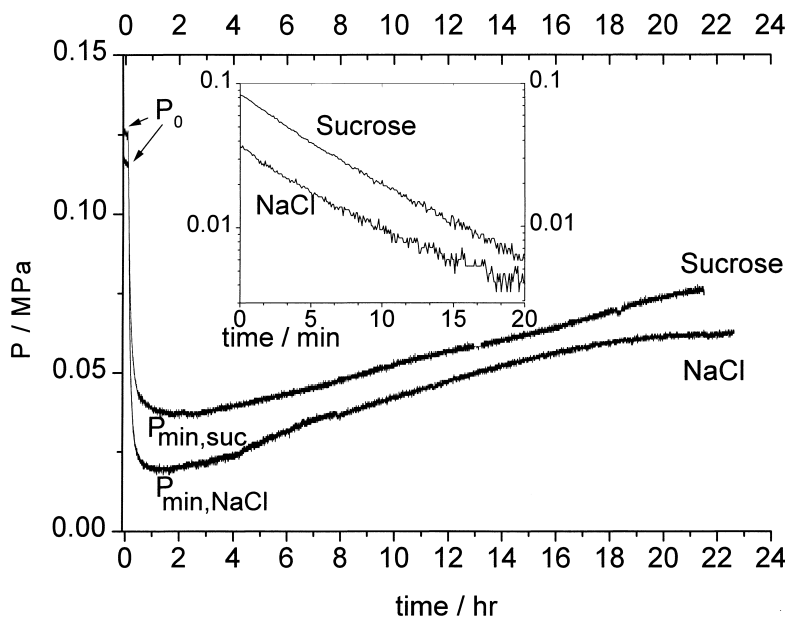


Fig. 4. A typical biphasic hyperosmotic turgor pressure response of a *V. utricularis* cell induced by addition of 46 mosmol kg⁻¹ NaCl and 49 mosmol kg⁻¹ sucrose, respectively, to ASW (pH = 8.1, $\pi_e = 2.83$ MPa). The initial turgor pressure, P_0 , relaxed to P_{\min} ; subsequently, turgor pressure upregulation occurred. *Inset:* half-logarithmic plot of the data of the first phase of the regulation, which can be attributed to water exchange (NaCl: $\tau_1 = 5.1$ min and sucrose: $\tau_1 = 8.5$ min). The second, very slow regulation phase is related to ion shifting (for details, see text).

frequently observed when the perfusion setup was switched on and can, therefore, be neglected.

From these and other experiments it appears that an offset turgor pressure exists in *V. utricularis* that is obviously generated by the vacuolar mucopolysaccharides. Support for this explanation was found by similar experiments on the pond water alga *Chara corallina* (data not shown). The vacuole of this species did not contain mucopolysaccharides as demonstrated by injection of alcian blue solution. Consistently, no offset turgor pressure could be recorded when the osmotic pressure of the external medium was matched to the osmotic pressure of the vacuole.

EFFECTS OF EXTERNAL SOLUTES ON TURGOR PRESSURE RELAXATION

Hyperosmotic Conditions

In the first set of experiments, turgor pressure relaxations of the algae were studied under hyperosmotic conditions. A typical example is shown in Fig. 4. The hyperosmotic turgor pressure relaxation was induced by replacement of ASW (pH = 8.1, osmotic pressure, $\pi_e = 1131$ mosmol kg⁻¹ = 2.83 MPa) by ASW + 46 mosmol kg⁻¹ NaCl ($\pi_e = 1177$ mosmol kg⁻¹ = 2.94 MPa). The down-relaxation phase of the turgor pressure regulation process could be fitted by a single exponential curve. From the half-logarithmic plot of the data (see inset of Fig. 4) the time constant, τ_1 , was determined to be 5.1 min (average value 9.4 ± 3.6 min; $n = 17$); a quasi-stationary value, $P_{\min,NaCl}$, was reached after about 40 min. These values were in very good agreement with the literature (Zimmermann et al., 1969), thus indicating that this phase of turgor pressure relaxation was solely due to an outwardly directed net water flow.

The water exchange phase was followed by a very slow, but continuous upregulation of turgor pressure (Fig. 4) mediated apparently by ion transport (Zimmermann et al., 1969; Heidecker et al., 2003). Rough approximation of the upregulation phase by an exponential curve (not shown) yielded a value of $\tau_2 = 420$ min for the time constant. The average value was determined to be 336 ± 148 min ($n = 7$). The large standard deviations of the time constants indicated that the cell-to-cell variation in the time course of the pressure upregulation was quite considerable. Even after 2 days, reestablishment of the original turgor pressure could only be recorded in a few cases. This was in contrast to findings observed for nonimpaled cells. Insertion of the pressure probe into these cells after 2 d of incubation in the hyperosmotic medium demonstrated that the original turgor pressure was nearly restored (data not shown; see also below). Impalement of the cells with microcapillaries apparently limited the long-term regulatory functions of the algae. We also found that (irreversible) changes of the uniform distribution of chloroplasts occurred after about 20 h under these conditions. In contrast, short-term osmotic manipulations were always reversible (see e.g., Fig. 5).

From the turgor pressure relaxation in Fig. 4 the reflection coefficient of NaCl was calculated to be $\sigma_{eNaCl} = 0.93$ by using Eq. 1 ($\varepsilon = 22.6$ MPa; $\pi_{i0} = 2.98$ MPa). A comparable value was found for KCl ($\sigma_{eKCl} = 0.91$). A similar biphasic hyperosmotic response was observed when the ASW was replaced by ASW + 49 mosmol kg⁻¹ sucrose ($\pi_e = 2.95$ MPa). Calculations of σ_{eSuc} from the half-logarithmic plot of the downrelaxation phase (inset of Fig. 4) yielded a value of 0.83 using appropriate values for ε and π_{i0} . This value was apparently less than the corresponding value for NaCl and significantly

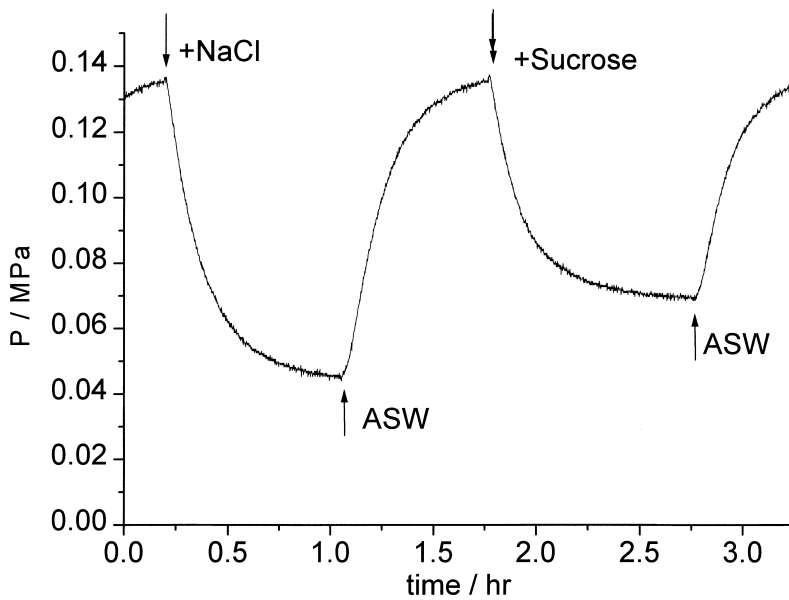


Fig. 5. Typical hyperosmotic turgor pressure response of an individual *V. utricularis* cell subjected successively to ASW + NaCl ($\pi_e = 2.946$ MPa), ASW, ASW + sucrose ($\pi_e = 2.942$ MPa) and ASW (indicated by *arrows*). Note that the original turgor pressure value was reestablished when the hyperosmotic solutions were replaced by ASW.

Table 1. Summary of internal and external reflection coefficients (σ_i and σ_e , respectively) measured on *Valonia utricularis* for different osmotica under various conditions

Osmotica	Reflection Coefficients					
	Preincubation in ASW				Preincubation in ASW medium containing sucrose (ASW _{suc,230})	
	Hyperosmotic		Hyposmotic		Hyperosmotic	Hyposmotic
	σ_i	σ_e	σ_i	σ_e	σ_e	σ_e
KCl	0.63 ± 0.13 (4)	0.91 ± 0.13 (5)	0.73 ± 0.35 (3)	n.d.	n.d.	n.d.
Sucrose	0.58 ± 0.17 (4)	0.86 ± 0.09 (6)	n.d.	n.d.	0.72 ± 0.15 (6)	0.63 ± 0.09 (5)
NaCl	n.d.	0.94 ± 0.05 (12)	n.d.	0.86 ± 0.09 (9)	0.78 ± 0.14 (6)	0.70 ± 0.17 (5)
PEG6000	n.d.	0.58 ± 0.08 (4)	n.d.	n.d.	n.d.	n.d.

The values were calculated from the pressure response to osmotic challenges. In parentheses, the number of experiments.

smaller than unity quoted in the literature for biological membranes including *V. utricularis* (Stein, 1967; Zimmermann & Steudle, 1970; Berestovsky, Ternovsky & Kataev, 2001). On average, σ_{eNaCl} and σ_{esuc} were 0.94 and 0.86, respectively (see also Table 1), indicating strongly that sucrose apparently has a lower reflection coefficient than NaCl. This finding was confirmed by experiments on individual cells subjected to ASW + NaCl followed by an ASW + sucrose regime. In the experiment of Fig. 5, ASW (1135.6 mosmol kg⁻¹ = 2.839 MPa) was replaced first by ASW + NaCl (1178.2 mosmol kg⁻¹; $\Delta\pi_e = 0.1065$ MPa, *arrow*). After reaching a quasi-stationary turgor pressure, the alga was exposed again to ASW (*arrow*) and then to ASW + sucrose (1176.8 mosmol kg⁻¹; $\Delta\pi_e = 0.1030$ MPa; *double-headed arrow*). Subsequent replacement by ASW resulted in the restoration of the original turgor pressure, indicating again that the turgor pressure changes were

reversible. From the turgor pressure relaxation curves σ_{eNaCl} and σ_{esuc} were calculated to be 1.00 and 0.76, respectively. Similar measurements on six different algae yielded an average σ_e value of 0.86 ± 0.09 for sucrose and 0.94 ± 0.05 for NaCl ($n = 12$; see also Table 1). Analogous measurements with PEG 6000 yielded a value of $\sigma_{ePEG} = 0.58 \pm 0.08$ ($n = 4$).

The reflection coefficients of sucrose and NaCl decreased significantly when cells were pre-equilibrated for 2 d in ASW_{suc,230}. The average σ_e values deduced from 6 pressure relaxation curves (induced by addition of about 40 mosmol kg⁻¹ NaCl or sucrose) were 0.78 ± 0.14 for NaCl and 0.72 ± 0.15 for sucrose (Table 1).

Hyposmotic Conditions

Turgor pressure response was also biphasic when the algae were subjected to ASW with reduced NaCl

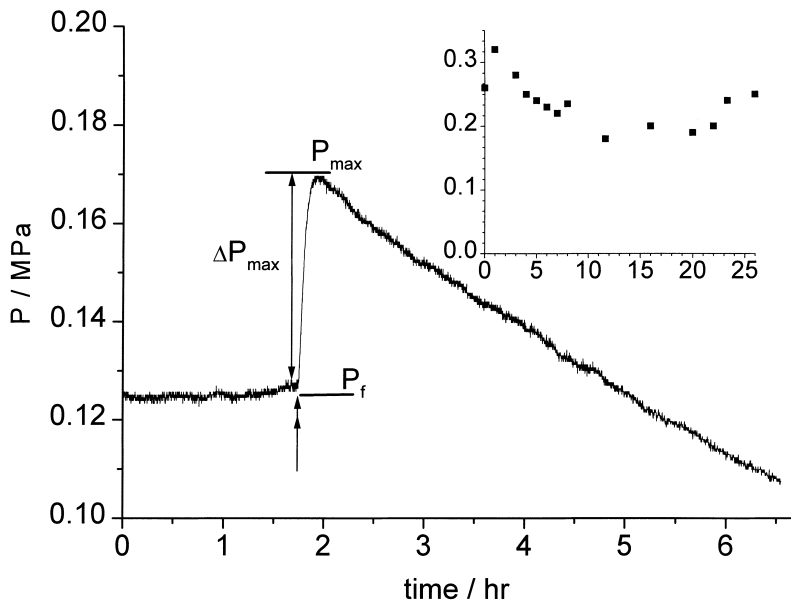


Fig. 6. A typical 'hyposmotic' turgor pressure response of a *V. utricularis* cell induced by isosmotic replacement of ASW ($\pi_e = 2.83$ MPa) by ASW in which an osmotically equivalent NaCl concentration was replaced by sucrose (i.e., $-\Delta\pi_{\text{eNaCl}} = +\Delta\pi_{\text{esuc}}$; ASW_{suc,227}). Note that the turgor pressure increased exponentially from 0.127 MPa to 0.169 MPa (corresponding to $\Delta P_{\text{max}} = 0.042$ MPa). The time constant was $\tau_1 = 3.3$ min, indicating that this phase was controlled by water shifting. Water exchange was followed by a slow backward regulation of turgor pressure towards values significantly below the original value. *Inset:* Response of turgor pressure determined on individual cells of *V. utricularis* after transfer from ASW in ASW_{suc,200} ($\pi_e = 2.83$ MPa). Note that in this case turgor pressure regulation consisted of three phases. The first two phases are qualitatively identical to the data measured for a single cell. The onset of the third phase, which results in the restoration of the original value, is not seen during 'hyposmotic' turgor pressure relaxation because of problems arising from long-term impalement (*see text*).

concentrations. The osmotic pressure was adjusted to final osmolalities of 2.67 MPa to 2.75 MPa by dilution with distilled water. From the exponential turgor pressure relaxation and subsequent downregulation (*data not shown*) τ_1 and τ_2 were calculated to be 8.1 ± 4.3 min ($n = 14$) and 301 ± 166 min ($n = 8$), respectively. These values agreed well with the time constants of hyperosmotic turgor pressure regulation.

Calculations of the reflection coefficient of NaCl from the water exchange phase yielded an average value of 0.86 ± 0.09 ($n = 9$). This value was significantly smaller than under hyperosmotic conditions (Table 1). However, consistent with hyperosmotic regulation, the reflection coefficient of NaCl decreased further when cells were pre-equilibrated in ASW_{suc,227} for 2 d. Such cells also allowed the determination of σ_e for sucrose because hyposmolality could be induced by removal of an equivalent amount of sucrose (or NaCl) from the medium. The average σ_e values ($n = 5$) of the pre-incubated cells were 0.70 ± 0.17 for NaCl and 0.63 ± 0.09 for sucrose. These values are also smaller than under hyperosmotic conditions (Table 1).

Isosmotic Conditions

An 'anomalous' turgor pressure regulation was induced when an osmotically equivalent concentration of NaCl in the ASW was replaced by sucrose (i.e., $-\Delta\pi_{\text{eNaCl}} = +\Delta\pi_{\text{esuc}}$). A typical example out of 44 experiments is shown in Fig. 6. As indicated in the figure, ASW was exchanged against ASW_{suc,227} after about 100 min. Despite isosmolality, the turgor pressure increased exponentially from 0.127 MPa to 0.169 MPa ($\Delta P_{\text{max}} = 0.042$ MPa) with a time constant of $\tau_1 = 3.3$ min (average value 5.1 ± 2.7 min;

$n = 23$). These values corresponded to the water exchange time. However, in contrast to hyper- and hyposmotic conditions, the downregulation was almost linear (Fig. 6), resulting in pressure values that were significantly lower than the original turgor pressure. Turgor pressure measurements on individual (non-impaled) cells incubated in isosmotic ASW_{suc,200} confirmed the above results (*see inset of Fig. 6*), but they also showed that after the downregulation of the turgor pressure below the initial value of 0.25 MPa, upregulation occurred with restoration of the original value after about 1 d.

The magnitude of the first ('hyposmotic') response depended on the sucrose concentration in ASW_{suc}. A plot of the ΔP_{max} values versus $\Delta\pi_{\text{esuc}}$ yielded a straight line (Fig. 7). This is expected because of $\Delta P_{\text{max}} = -(-\sigma_{\text{eNaCl}} \cdot \Delta\pi_{\text{eNaCl}} + \sigma_{\text{esuc}} \cdot \Delta\pi_{\text{esuc}}) = (\sigma_{\text{eNaCl}} - \sigma_{\text{esuc}}) \Delta\pi_{\text{esuc}}$. Thus, it is evident that the slope of 0.053 (regression coefficient $r = 0.89$) of the straight line must be equal to the difference in the two reflection coefficients and that σ_{esuc} must be smaller than σ_{eNaCl} . The effect of isosmotic ASW_{suc} on the turgor pressure was pH-dependent (*data not shown*). When the pH was lowered to 4.5, the 'hyposmotic' turgor pressure response decreased significantly (e.g., 0.011 MPa in the case of 1.05 MPa sucrose [*not shown*] instead of 0.039 MPa at pH 8.1, *see Fig. 7*).

Isosmotic replacement of NaCl in ASW (pH = 8.1) by mannitol, glucose, sorbitol, trehalose, PEG (MW about 1000 Da), dextran (MW = 4000 Da to 6000 Da) as well as by NaMES yielded similar results as with sucrose (Fig. 7), although their reflection coefficients should be $\sigma_e = 1$. When PEG of a molecular weight of 2000 Da or 6000 Da was used, the 'hyposmotic' response of turgor pressure was

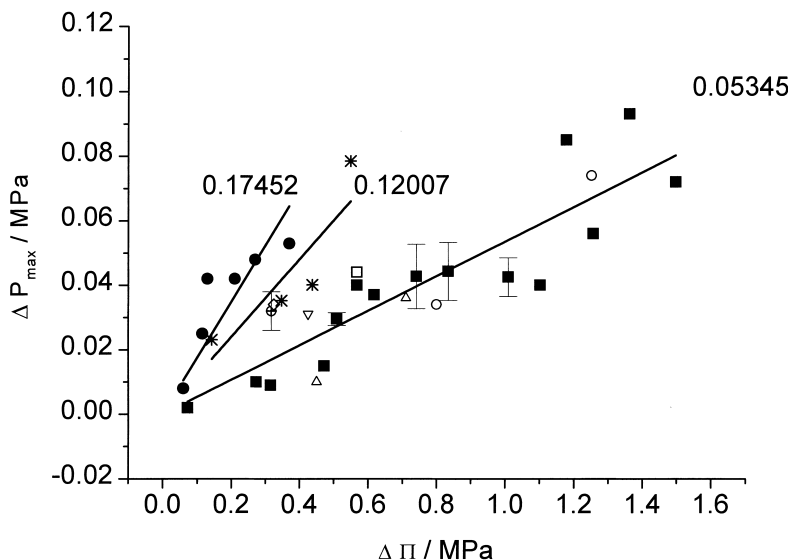


Fig. 7. Plot of the ΔP_{\max} values as a function of the osmotic pressure component arising from sucrose (■) and PEG (PEG 2000: *, PEG 6000: ●) in ASW. Data points were obtained as described in Fig. 6 and fitted by linear regression ($r = 0.89$ for sucrose). The dimensionless slope of the straight line corresponding to $(\sigma_{\text{eNaCl}} - \sigma_{\text{esuc}})$ was 0.053 (for further explanation, see text). The open symbols represent the following solutes: mannitol: (○), glucose: (+), sorbitol: (◇), dextran: (▽), trehalose (□) and MES: (△). Some of the data points represent mean values ($n = 3 \pm \text{SD}$).

even more pronounced (Fig. 7). Calculations showed that the average σ_{e} value of PEG 6000 was 0.58 ± 0.08 ($n = 4$). This value could also be deduced from hyperosmotic experiments in which the same alga was subjected to repeated regimes of ASW + NaCl and ASW + PEG (*data not shown*).

In contrast to the above solutes, isosmotic substitution of NaCl by KCl, Na-gluconate, acetamide, glycine and urea did not result in a turgor pressure increase. In these cases there was a slight, very slow turgor pressure decrease or no change (*data not shown*). Consistently, no hyperosmotic turgor regulation was observed upon addition of these solutes to ASW, indicating that the apparent σ_{e} values of these solutes must be comparable to σ_{eNaCl} .

EFFECTS OF EXTERNAL SUCROSE ON THE TURGOR PRESSURE OF *CHARA CORALLINA*

At first glance, the pond water alga *C. corallina* shows a similar ‘anomalous’ turgor pressure response under isosmotic conditions as the marine alga *V. utricularis*. However, a closer inspection of the data shows notable differences between the two species. A typical turgor pressure relaxation recording out of 22 experiments is shown in Fig. 8. As mentioned in Materials and Methods, demonstration of the effect required that the original turgor pressure of about 0.47 MPa was pre-lowered to 0.1 MPa by addition of APW + 160 mosmol kg^{-1} NaCl (*not shown*). Consistent with the literature (Tyerman & Steudle, 1984), the exponential downrelaxation of the turgor pressure by water exchange occurred with a relaxation time of $\tau = 20.8$ s; the final pressure, P_{f} , was reached after about 150 s. In contrast to *V. utricularis*, but in agreement with the literature (Kamiya & Tazawa, 1956; Bisson et al., 1995), subsequent upregulation of turgor pressure due to solute exchange did not occur. As indicated in Fig. 8, when the NaCl in the saline

APW was replaced by an osmotically equivalent concentration of sucrose, a ‘hypoosmotic’ pressure response was recorded that increased linearly with increasing sucrose concentration (*see inset of Fig. 8*). The slope of the straight line ($r = 0.94$) was with 0.091 significantly larger than in the case of *V. utricularis*, suggesting that σ_{esuc} was apparently much smaller than σ_{eNaCl} . However, in contrast to *V. utricularis*, pressure relaxed very rapidly back to the original value. This finding demonstrates very clearly that σ_{esuc} must be equal to σ_{eNaCl} for cells of *C. corallina*. Delayed equilibration between the bulk solution and the cell wall obviously prevents the instantaneous development of the full osmotic pressure of sucrose close to the membrane barrier. The much larger time constant of downrelaxation of turgor pressure in *V. utricularis* suggests that, apart from unstirred layer effects, other interferences of the organic osmolytes with the wall-membrane barrier of this alga must occur.

Time constants of the biphasic response in turgor pressure of *C. corallina* showed quite a large variability that could not be correlated with the sucrose concentration. Pooling of the data yielded average values for τ_1 of 5.9 ± 3.4 s ($n = 15$) and for τ_2 of 25.9 ± 20.5 s ($n = 13$). Despite the large variations, it is obvious that pressure downrelaxation occurred with a time constant in the range measured for water exchange upon NaCl treatment (*see above and below*). Pressure uprelaxation was apparently also induced by water inflow, but was much faster than expected from the time constant of water exchange. This could be due to (variable) concentration effects between the two membranes arranged in series, induced by the sucrose treatment. Such effects can lead to a polarity in water transport (i.e., the hydraulic conductivity for endosmotic flow is larger than for exosmotic flow and thus $\tau_1 < \tau_2$), provided that the reflection coefficients of the two membranes of the

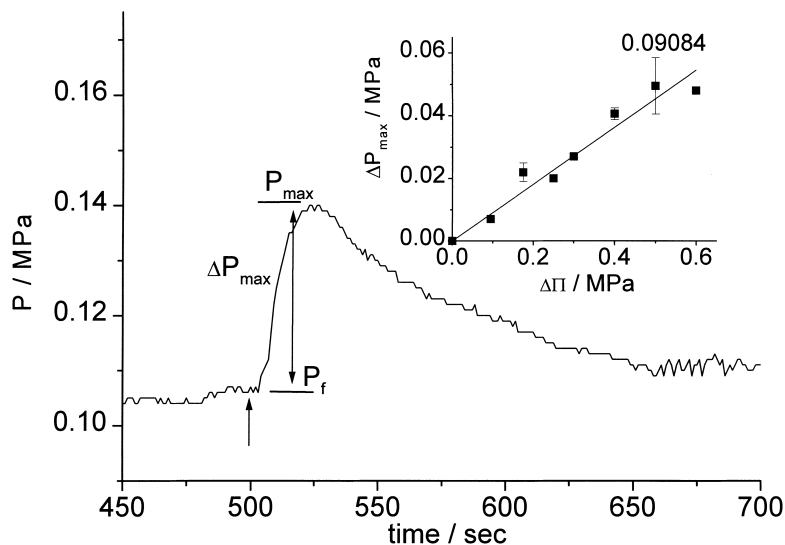


Fig. 8. A typical ‘hyposmotic’ turgor pressure response of a cell of the pond water alga *Chara corallina* induced by sucrose under isosmotic conditions. Experimental conditions were identical to those in Fig. 6 except that the original turgor pressure of 0.47 MPa was lowered to about 0.1 MPa by addition of 0.40 MPa NaCl to the artificial pond water (APW; $\pi_c = 0.02$ MPa). Note that the alga responded with an increase in turgor pressure ($\Delta P_{\max} = 0.034$ MPa) due to water exchange (see text), but that (in contrast to *V. utricularis*) the pressure relaxed back to the original, pre-set value with a similar time constant. *Inset:* plot of ΔP_{\max} as a function of the osmotic pressure component arising from sucrose in APW + NaCl. Data points were fitted by linear regression ($r = 0.94$). The dimensionless slope of the straight line was 0.091. Some of the data points represent mean values ($n = 3 \pm \text{sd}$).

composite barrier are different, (see Kedem & Katchalsky, 1963; Tazawa & Kiyosawa, 1973; Zimmermann & Steudle, 1974, 1978). Consistent with this explanation, subsequent replacement of APW + 168 mosmol kg^{-1} sucrose by APW resulted in the complete reestablishment of the original turgor pressure of 0.47 MPa, whereby the time constant was again in the range of the time constant for water outflow (23.4 ± 6.5 s; $n = 16$).

EFFECTS OF VACUOLAR SOLUTES ON TURGOR PRESSURE RELAXATION OF *V. UTRICULARIS*

The vacuolar reflection coefficients of electrolytes and non-electrolytes, σ_i , of *V. utricularis* were determined from turgor pressure relaxations induced by perfusing the vacuole with media of various osmolality while keeping the osmolality of the ASW constant. Under these conditions, cell wall effects are excluded, but the full impact of the multiply-folded tonoplast on the determination of the reflection coefficients should be seen.

Hyperosmotic Conditions

A representative hyperosmotic experiment performed on a perfused *V. utricularis* cell is shown in Fig. 9. Perfusion intervals are marked with arrows in the figure. After perfusion with AVS₁₂₀₈ and release of the pressure clamp of 0.120 MPa, the pressure relaxed exponentially to a new quasi-stationary turgor pressure value of 0.133 MPa. Subsequently the cell was clamped to this pressure value for 1 h. During this clamp, AVS was replaced by perfusing the vacuole with AVS to which 62 mosmol kg^{-1} (=0.155 MPa) KCl was added. After the release of the clamp, the typical biphasic turgor pressure response was observed. The exponential turgor pressure increase

($\tau_1 = 10.7$ min) was followed by an exponential downregulation ($\tau_2 = 209$ min). On average, the time constants of the two phases were $\tau_1 = 11.1 \pm 2.5$ min ($n = 8$) and $\tau_2 = 247 \pm 36$ min ($n = 4$), respectively. Both time constants are in the range measured for turgor pressure relaxation and subsequent regulation induced externally.

By using the relevant parameters, the reflection coefficient of KCl was calculated to be $\sigma_{i\text{KCl}} = 0.63 \pm 0.13$ ($n = 4$). A similar hyperosmotic response was observed when the AVS was replaced by AVS to which 42 mosmol kg^{-1} sucrose ($\Delta\pi_i = 0.105$ MPa) was added. Calculation of $\sigma_{i\text{suc}}$ yielded a value of 0.58 ± 0.17 ($n = 4$). It is evident that $\sigma_{i\text{KCl}} > \sigma_{i\text{suc}}$, but that the absolute values of the reflection coefficients of both solutes were considerably lower than those determined from external osmotic manipulations (see also Fig. 5) even though interference of the solutes with the cell wall was eliminated.

Hyposmotic Conditions

After equilibration with AVS ($\pi_{i0} = 1210$ mosmol kg^{-1}), the cell was subjected to the same perfusion/clamp regime as in Fig. 9 except that AVS with reduced KCl concentration (osmolality range $\pi_{i0} = 1120$ to 1170 mosmol kg^{-1}) was used. The time constant of the turgor pressure relaxation was similar ($\tau_1 = 8.7 \pm 4.9$ min; $n = 8$) to the corresponding value measured under hyperosmotic conditions. However, no subsequent upregulation was observed. The reflection coefficient $\sigma_{i\text{KCl}}$ (0.73 ± 0.35 ; $n = 3$) was larger than the ‘hyperosmotic’ value (Table 1).

Isosmotic Conditions

Using the same initial perfusion regime, but replacing various amounts of KCl by isosmotic concentrations

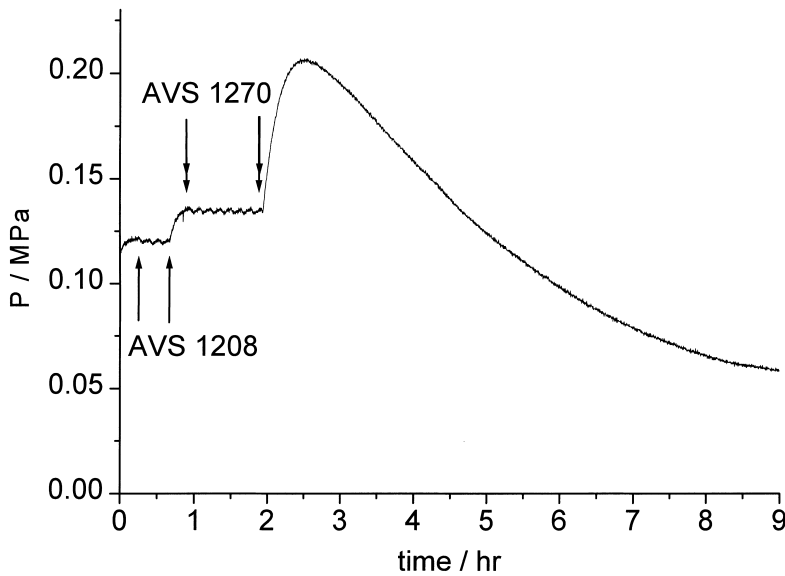


Fig. 9. A typical hyperosmotic turgor pressure response of a *V. utricularis* cell induced by vacuolar addition of 0.155 MPa KCl. The alga was bathed in ASW ($\pi_e = 2.83$ MPa) and perfused with AVS ($\pi_i = 3.02$ MPa) at a clamped pressure of 0.12 MPa (single-headed arrows). Then the pressure was released and a new turgor pressure equilibrium was established at 0.133 MPa after about 40 min. This pressure was clamped (double-headed arrows) and the vacuole perfused with AVS + KCl. Subsequent release of the pressure resulted in a biphasic response. The time constants ($\tau_1 = 10.7$ min and $\tau_2 = 209$ min) correspond well to those deduced from externally-induced pressure regulations (hyposmotic: see text and hyperosmotic: see Fig. 4).

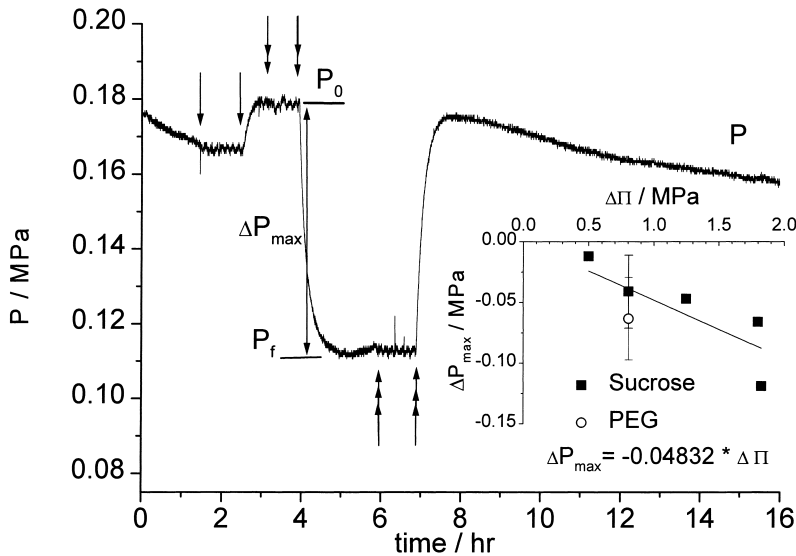


Fig. 10. A typical 'hyposmotic' turgor pressure response of a perfused *V. utricularis* cell induced by isosmotic replacement of AVS (1210 mosmol kg^{-1}) by AVS in which an osmotically equivalent KCl concentration was replaced by sucrose (i.e., $-\Delta\pi_{\text{KCl}} = +\Delta\pi_{\text{suc}}$; AVS_{suc,380}). The same perfusion/clamp regime was used as described in Fig. 9 except that turgor pressure was clamped for a third time (triple-headed arrows) to P_f . During this clamp, the cell was perfused with AVS before the pressure was released again. The

of sucrose (osmolality range $\pi_{i0} = 32$ to 720 mosmol kg^{-1}) an exponential 'hyposmotic' response was observed upon release of the clamped pressure (Fig. 10). A new steady-state pressure, P_f , was reached after 1 h; the time constant of the relaxation process was $\tau_1 = 11.9$ min (mean value $\tau_1 = 14.3 \pm 7.8$ min; $n = 5$) and thus in agreement with the water exchange data in Figs. 5 and 9. In contrast to 'true' hyposmotic conditions, subsequent upregulation of the pressure was not observed when the sucrose

pressure relaxed back to the original value with a time constant of $\tau_1 = 9.6$ min, i.e., by water exchange. *Inset:* Plot of the ΔP_{max} values as a function of the osmotic pressure component arising from sucrose in AVS (filled squares). Data points were fitted by linear regression ($r = 0.75$). The absolute value of the dimensionless slope of the straight line was -0.048 . Empty circles (O) represent the mean ΔP_{max} values ($n = 4 \pm \text{SD}$) recorded when vacuolar KCl was replaced by 0.81 MPa PEG 6000.

concentration was larger than 40 mosmol kg^{-1} (as in Fig. 10, perfusion with AVS_{suc,380}). This was not due to irreversible damage of the cells, as shown by clamping of P_f and perfusion with AVS (triple-headed arrows). Upon release of the clamp, the original turgor pressure was reestablished within $\tau_1 = 9.6$ min (mean value $\tau_1 = 14.9 \pm 9.3$ min; $n = 3$).

As in the case of external manipulation of the medium (Fig. 6), the vacuolar 'hyposmotic' response depended on the sucrose concentration (inset of Fig.

10). Despite the large scatter of the data, a linear function between the ‘hyposmotic’ response and sucrose seemed to exist. The scatter of the data probably resulted from the relatively slow exchange rate of AVS with sucrose-containing AVS. The slope of the straight line ($r = 0.75$) had a similar magnitude (-0.048) as the slope of the straight line in Fig. 7 for externally replaced sucrose. The absolute value of the slope of the straight line corresponding to $\sigma_{iKCl} - \sigma_{isuc}$ was calculated to be 0.05, indicating that even for vacuolar manipulations $\sigma_{iKCl} > \sigma_{isuc}$.

Isosmotic replacement of vacuolar KCl by PEG 6000 resulted also in a ‘hyposmotic’ response (inset in Fig. 10). Because of viscosity problems and of the limits of accuracy only a concentration of 0.81 MPa could be tested. The induced pressure change seemed to be smaller than under external replacement conditions and more comparable to that of sucrose ($\sigma_{iPEG} = 0.56$).

Vacuolar Reflection Coefficient of KCl Derived from Water Relation Parameters under Steady-state Conditions

In contrast to sucrose and PEG, isosmotic exchange of KCl by NaCl did not induce a turgor pressure change in perfused cells (*data not shown*), indicating that the σ_i values of both electrolytes were identical. Because of this and the knowledge of σ_{eKCl} , the internal reflection coefficient of KCl can also be calculated from the equilibrium turgor pressure and the internal osmotic pressure of cells kept in ASW. By using Eq. 3, σ_{iKCl} was determined to be 0.90 ± 0.02 ($n = 15$). When cells were incubated for 2 d in ASW_{suc,230}, the values for turgor and osmotic pressure of the vacuolar sap were similar to those in ASW, indicating that both σ_e and σ_i were unaltered. A comparison of these data with the results obtained from internally- and externally-induced turgor pressure relaxations (*see above*) shows (1) that 2 d exposure to sucrose has apparently no effect on σ_{iKCl} , (2) that the σ_{iKCl} values were significantly higher than those derived from turgor pressure manipulation and (3) that they were comparable to those of the external reflections coefficients σ_{eNaCl} and σ_{eKCl} .

Discussion

Reflection coefficients, σ , have been used for determining whether a common water-solute transporting pathway exists. Values of σ between zero and one have been taken as evidence for coupling between water and solute flow (Kedem & Katchalsky, 1958; Katchalsky & Curran, 1965). In the theory of Kedem & Katchalsky (1958), the mechanism of osmotic water flow is not specified but is assumed to be identical to that for pressure-driven flow. If diffusive

and hydraulic (viscous) flow components are involved, $\sigma < 1$ does not necessarily imply water-solute interactions in permeable aqueous channels. Indeed, the osmotic features of water channels such as aquaporins (Kaldenhoff & Eckert, 1999), which are impermeable to most small solutes, can be explained by changes in the mechanism of water flow in regions either accessible or inaccessible to solute, created by a varying cross-section of the channel (Curry et al., 2001).

There is still no clear-cut evidence that aquaporins exist or are temporarily expressed during turgor pressure regulation in *Valonia utricularis* or other pond and marine algae. However, measurements of the diffusional permeability, P_d (cm s^{-1}) and of the hydraulic conductivity, L_p , on cells of *V. utricularis* have shown (Gutknecht, 1968) that $P_d = L_p RT/V_w$ (R = gas constant, T = temperature and V_w = partial molar volume of water). This agreement suggests that water flow through the entire wall-membrane barrier is diffusional and that any hydraulic component is negligible. From this point of view the concept of Kedem & Katchalsky (1958) modified by Zimmermann & Steudle (1974) for derivation of reflection coefficients and other water relation parameters from turgor pressure relaxations can be applied to *V. utricularis*.

Determination of reflection coefficients for giant alga cells (as well as for cells and tissues of higher plants) with the pressure probe circumvents the method-dependent artifacts found with adherent and suspended animal cells (Toon & Solomon, 1996; Verkman, 2000). However, the principal challenges in the calculation of accurate σ values for algae, plant cells and tissues from turgor pressure relaxation curves are to define the effective surface area of the serial membrane barriers to water transport, and to determine the effects of unstirred layers on the measured water fluxes. Unstirred layer effects and surface are not independent of each other (Richardson, Licko & Bartoli, 1973; House, 1974; Barry & Diamond, 1984; Verkman & Dix, 1984; Verkman, 2000). The effect of an unstirred layer surrounding a smooth spherical membrane increases as the cell radius increases. If the exchange area of water and solute is greatly increased by membrane infolding, unstirred layer effects increase and become difficult to quantify. A theoretical analysis of flows through folded membrane has shown (Richardson et al., 1973) that, close to osmotic equilibrium, water flow can increase by several times the increase in area while salt flow only increases by a fraction of it.

The calculations of vacuolar and external reflection coefficients for *V. utricularis* (and for *Chara corallina*) from turgor pressure relaxation experiments reported above were made on the basis of the equations derived by Zimmermann & Steudle (1974) in the light of the thermodynamics of irreversible

processes (Katchalsky & Curran, 1965). The analysis is based (among other things) on the assumptions that the surface area of the serially arranged tonoplast and plasmalemma are planar (allowing the two membranes to be treated as a single barrier) and that intravacuolar and extracellular unstirred layer effects are negligible.

The data presented here demonstrate that the assumptions may be valid for *C. corallina*. In the pond water alga the cytoplasm layer is clearly separated from the tonoplast and the plasmalemma (Franceschi & Lucas, 1980). Both membranes are planar. The alga displays an extensive cytoplasmic streaming (Kamiya, 1986) that stirs its cytoplasm by moving water, solutes and organelles around. Because of frictional and hydraulic coupling, the layer at the inner surface of the central vacuole is presumably also stirred to some extent (as is known from cell electrorotation; Fuhr, Zimmermann & Shirley, 1996). We found no indications that the vacuolar sap contained mucilage or related compounds. The vacuolar sap can apparently be treated as a 'dilute' solution. Only the cell wall of *C. corallina* must be considered a compartment in which unstirred layers occur. As demonstrated here by pressure probe measurements, water inflows of varying magnitude could be induced by isosmotic exchange of appropriate concentrations of NaCl against sucrose (Fig. 8). This finding could lead to the interpretation that $\sigma_{\text{esuc}} < \sigma_{\text{eNaCl}}$. However, the pressure responses were only transient and apparently resulted from slow diffusion of the sucrose into the wall (effects that were ignored by Berestovsky et al. [2001] in their work on isolated walls of *C. corallina*). Within about 50 s the original turgor pressure was restored by water outflow. As already mentioned above, this can be taken as evidence that sucrose in the bulk solution has apparently equilibrated with the cell wall and that σ_{esuc} is nearer unity and equal to σ_{eNaCl} , as expected if small unstirred layer effects under steady-state conditions are taken into account (Dainty & Ginzburg, 1963; Barry & Hope, 1969). Thus, we can conclude that intra- as well as extracellular unstirred layers are of secondary importance in this giant pond water alga.

However, the assumptions are not valid for the marine alga *V. utricularis*, which apparently favors the strategy of preventing convection and restricting diffusion by generating huge intracellular unstirred layers in addition to the extracellular ones linked to the cell wall. Clearly, the mucilage network seen in *V. utricularis* (Fig. 2) creates unstirred layer effects in the huge central vacuole, which occupies more than 95% of the cell volume. Due to the negative charges of the mucopolysaccharides, water exists as polarized multilayers extending far beyond the one or two layers of water molecules conventionally considered (see, e.g., Clegg, 1982; Barry & Diamond, 1984; Esch

et al., 1999). The cation-exchanging mucopolysaccharide filaments are apparently one adaptation of *V. utricularis* to the fluctuating vacuolar ion concentrations (e.g., of Ca^{2+}) resulting from moderate natural osmotic changes in sea water. The vacuolar mucopolysaccharides may also act as scaffolding to stabilize the tonoplast and delay complete turgor pressure loss as they decrease the chemical activity of water (equivalent to a turgor pressure of about 17 kPa as measured by the pressure probe).

Surprisingly, no extracellular mucilage could be found for cells of *V. utricularis*, unlike for the salt-tolerant alga *Lamprothamnium papulosum* (Shepherd & Beilby, 1999; see also the literature quoted there). In contrast to *V. utricularis*, this alga inhabits estuaries and coastal pools where the salinity is extremely variable. As in the case of *C. corallina*, the cell interior is stirred relatively well by cytoplasmic streaming. *L. papulosum* forms external mucilage, enhancing external unstirred layer effects, to delay the full impact of ambient ion fluctuations on membrane and cytoplasmic processes. Such external mucilage layers are apparently unnecessary for the cells of *V. utricularis* because the unstirred layer region is 'displaced' into the cytoplasm by multiple infoldings of the tonoplast and the resulting spongy architecture of the cytoplasm (Fig. 1). The innumerable tonoplast infoldings (approaching to within 40 nm of the plasmalemma and surrounding the cytoplasmic strands) form a continuum ideal for creating extended unstirred layers. The vacuolar reflection coefficients calculated for sucrose and PEG from turgor pressure relaxations (σ_{isuc} , $\sigma_{\text{iPEG}} = 0.58$) were even lower than that for KCl ($\sigma_{\text{iKCl}} = 0.63$ under hyperosmotic conditions and $\sigma_{\text{iKCl}} = 0.73$ under hyposmotic conditions). When σ_{iKCl} was determined from steady-state measurements, its value increased to 0.91 as expected because unstirred layer effects are greatest for rapid water movement through extended, poorly stirred compartments (see above).

Very low, 'short-term' σ_{iKCl} values make a great deal of sense because cytoplasm and vacuole osmotic pressure of *V. utricularis* can be unbalanced during turgor adaptation upon (externally induced) fluctuations in vacuolar salt concentration without generating a hydrostatic pressure differential across the tonoplast. Similarly, the structured (bound) water in the cytoplasmic strands (Clegg, 1982) may equally contribute to a delayed equilibration of the osmotic pressure in both compartments during turgor pressure regulation.

The effect of external unstirred layers bound to the cell wall on the 'short-term' reflection coefficients of KCl and NaCl of *V. utricularis* are much less ($\sigma_{\text{eKCl}} = 0.91$ and $\sigma_{\text{eNaCl}} = 0.94$; Table 1), but they are apparently not negligible, as was seen when organic osmolytes were applied. From the increase in turgor pressure observed when NaCl was replaced

isosmotically by an equivalent concentration of an organic osmolyte (Figs. 6 and 7), we can conclude that urea, acetamide and glycine (MW between 59 and 75 Da) have reflection coefficients similar to those of NaCl², whereas sucrose and trehalose (MW 342 Da) assumed smaller σ values (around 0.86) and PEG 6000, an even much smaller value (0.58). This seems to suggest that size-exclusion effects of the wall are exclusively responsible for limitation of permeation through the cell wall. However, the finding that MES (MW 195 Da), but not gluconate (MW 196 Da) evoked a turgor pressure increase when used for replacement of isosmolar concentrations of Cl⁻ showed that charge and/or steric effects must also be involved.

Interestingly, in contrast to *C. corallina*, equilibration between the bulk solution containing sucrose and the wall did apparently not occur. Downregulation of the turgor pressure was considerably slower than expected from the water exchange time constant. The time scale was more in the range recorded for turgor pressure regulations under hyposmotic conditions (even though the 'isosmotic' kinetics were more linear than exponential; see Fig. 6). This suggests that the decrease in turgor pressure was achieved mainly by efflux of vacuolar KCl, increasing the solute concentration at the wall/plasmalemma interface.

Severe restriction of diffusion of sucrose (and, probably, the other organic osmolytes) in the cell wall of *V. utricularis*, but not of *C. corallina* is probably due to differences in the crystallographic structures of the cell wall. High-resolution atomic force microscopy as well as infrared and electron diffraction studies of the wall of *V. macrophysa* and *Ventricaria ventricosa* (closely related with *Valonia*, both belonging to the *Cladophorales*) have shown (Hieta et al., 1994; Sugiyama & Okano, 1990; Sugiyama, Harada & Saiki, 1987; Baker et al., 1997) that each microfibril consists of more than thousand perfectly arranged cellulose chains oriented in a parallel fashion. Therefore, these algae are widely accepted as the source of a native cellulose I standard, having the highest known crystallinity.

Evidence that the peculiar cell wall structure of *Valonia* significantly limits permeation of solutes is given by the experiments in which isosmotic replacement of NaCl by sucrose was performed at pH 4.5. Under these conditions the pressure response was much smaller and backregulation faster than at pH 8.1, apparently because of a reduction of unstirred

layer effects due to the well-known effect of low pH on wall loosening (Cleland, 1971).

The low external and vacuolar σ values of *V. utricularis* can be explained by the effects of the unstirred layers related to the cell wall and the spongy architecture of the cytoplasm. However, effects arising from changes of the salt concentration or specific interactions of the organic osmolytes with the membranes cannot be completely excluded. Interactions of sucrose and other sugars (particularly of trehalose) with membranes are well-known (Crowe & Crowe, 1984, 2000; Koynova et al., 1997; Mussauer et al., 2001). These kosmotropic substances (water structure makers) favor—among other things—the formation of hexagonal phases (H_{II}) in lipid bilayers resulting in an increase of water conductance. Similar modulations of the lipid phase are also known from PEG- (and dextran-) induced cell-to-cell fusion (Arnold et al., 1985). Thus, such effects may also partly be responsible for the very small external (and also vacuolar) 'short-term' σ values of PEG (Table 1) and of dextran, even though long-term effects appear to be more likely. Consistent with this, preliminary ultrastructural studies on cells subjected to long-term sucrose exposure indicate changes in the organization of the cytoplasm (*our unpublished data*). Support for long-term effects of sucrose are also given by the finding reported here that 2 d pre-incubation of algae in solutions containing sucrose resulted in lower σ_e values for NaCl and sucrose when deduced from turgor pressure relaxations (0.78 ± 0.14 and 0.72 ± 0.15 , respectively). Despite this, recovery of the original turgor pressure apparently occurred in these cells, as suggested by the experiments under isosmotic conditions shown in the inset of Fig. 6. This could be taken as evidence that sucrose interacts with the plasmalemma and/or the cytoplasmic strands (in the long term) by increasing the hydraulic conductivity of the membranes.

To sum up, Verkman (2000) has recently rejected the concept of reflection coefficients and mandates reconsiderations because of method-dependent artifacts, unstirred layer effects and the presence of aquaporins (excluding solute transport). In the light of the considerations given above, we feel that, at least for plant cells, the determination of 'long-term' and 'short-term' reflection coefficients of solutes is obviously quite useful, provided that organic osmolytes are used to which the biomembrane is usually impermeable on a short time scale. When values lower than unity are found, this does not necessarily give information only about water-solute coupling. On this point we agree with Verkman (2000) and Curry et al. (2001). However, as shown here, lowered σ values can point to large unstirred layer effects arising from peculiar structures of the membranes and/or from the walls. Thus, measurements of σ values can complement simultaneous ultrastructural

² Zimmermann and Steudle (1970) reported much lower σ values for these organic osmolytes compared to those measured here. The reason for this is, that these authors determined the reflection coefficient on cells bathed in solutions containing very low concentrations of NaCl. This probably alters membrane properties, but yields σ values unaffected by high salt concentrations.

studies (which are not always free of artifacts). If the ultrastructure of a cell does not explain σ values in terms of unstirred layers, it is clear that we have to consider aquaporin effects as described by Curry et al. (2001) or found very recently by us for roots of higher plants. Split-root experiments showed (Schulze, Wegner, Binder, Sattelmacher, Haase, Kaldenhoff & Zimmermann, unpublished data) that ammonium and nitrate suppress and enhance, respectively, aquaporin expression, thus changing the hydraulic conductivity of the membrane barriers and, in turn, the reflection coefficients.

Even in cases where interpretation of σ values smaller than unity is not as straightforward as for *V. utricularis*, their knowledge is important in order to predict the direction and magnitude of the pressure response and regulation upon osmotic challenges. Otherwise, when ignoring reflection coefficients, pressure responses may be considered as anomalous, as shown here for isosmotic replacement pressure of NaCl by sucrose both for a marine and a pond water alga. Such effects must be kept in mind when salinity or other osmotic pressure experiments are performed on higher plants, provided that the data obtained here can be extrapolated. This seems to be the case for glycophytes (see Schneider, Zhu & Zimmermann, 1997).

This work was supported by a grant from the Deutsche Forschungsgemeinschaft (Zi 99/13-1). We are indebted to Prof. G. Krohne, Wurzburg, for technical support, his advice regarding the preparation and interpretation of the electron micrographs, and critical reading of the manuscript. We thank C. Gehrig and D. Bunsen for skilful technical assistance.

References

- Arnold, K., Herrmann, A., Pratsch, L., Gawrisch, K. 1985. The dielectric properties of aqueous solutions of poly(ethylene glycol) and their influence on membrane structure. *Biochim. Biophys. Acta* **28**:515–518
- Baker, A.A., Helbert, W., Sugiyama, J., Miles, M.J. 1997. High-resolution atomic force microscopy of native *Valonia* cellulose I microcrystals. *J. Struct. Biol.* **119**:129–138
- Barry, P.H., Diamond, J.M. 1984. Effects of unstirred layers on membrane phenomena. *Physiol. Rev.* **64**:763–872
- Barry, P.H., Hope, A.B. 1969. Electro-osmosis in membranes: effects of unstirred layers and transport numbers. *Biophys. J.* **9**:729–757
- Berestovsky, G.N., Ternovsky, V.I., Kataev, A.A. 2001. Through pore diameter in the cell wall of *Chara corallina*. *J. Exp. Botany* **52**:1173–1177
- Bisson, M.A., Kiegle, E., Black, D., Kiyosawa, K., Gerber, N. 1995. The role of calcium in turgor regulation in *Chara longifolia*. *Plant Cell Environ.* **18**:129–137
- Chamberlin, M.E., Strange, K. 1989. Anisomotic cell volume regulation: a comparative. *Am. J. Physiol.* **257**:C159–C173
- Chan, H.C., Nelson, D.J. 1992. Chloride-dependent cation conductance activated during cellular shrinkage. *Science* **257**:669–671
- Clegg, J.S. 1982. Alternative views on the role of water in cell function. In: Biophysics of water. F. Franks and S. Mathias, editors, pp. 365–383. Wiley, New York
- Cleland, R. 1971. Cell wall extension. *Ann. Rev. Plant Physiol.* **22**:197–222
- Crowe, J.H., Crowe, L.M. 1984. Preservation of membranes in anhydrobiotic organisms: the role of trehalose. *Science* **223**:701–703
- Crowe, J.H., Crowe, L.M. 2000. Preservation of mammalian cells — learning nature's tricks. *Nature Biotechnol.* **18**:145–146
- Curry, M.R., Shachar-Hill, B., Hill, A.E. 2001. Single water channels of Aquaporin-1 do not obey the Kedem-Katchalsky equations. *J. Membrane Biol.* **181**:115–123
- Dainty, J., Ginzburg, B.Z. 1963. The permeability of protoplasts of *Chara australis* and *Nitella translucens* to methanol, ethanol and isopropanol. *Biochim. Biophys. Acta* **79**:122–128
- Esch, M., Sukhorukov, V.L., Kurschner, M., Zimmermann, U. 1999. Dielectric properties of alginate beads and bound water relaxation studied by electrorotation. *Biopolymers* **50**:227–237
- Findlay, G.P. 2001. Membranes and the electrophysiology of turgor regulation. *Aust. J. Plant Physiol.* **28**:617–634
- Franceschi, V.R., Lucas, W.J. 1980. Structure and possible function(s) of Charasomes; complex plasmalemma-cell wall elaborations present in some Characean species. *Protoplasma* **104**:253–271
- Fuhr, G., Zimmermann, U., Shirley, S.G. 1996. Cell motion in time-varying fields: Principles and potential. In: Electromanipulation of Cells. U. Zimmermann and G.A. Neil, editors, pp. 259–328. CRC Press, Boca Raton
- Guggino, S.E., Gutknecht, J. 1982. Turgor regulation in *Valonia macrophysa* following acute hyposmotic shock. *J. Membrane Biol.* **67**:155–164
- Gutknecht, J. 1968. Permeability of *Valonia* to water and solutes: apparent absence of aqueous membrane pores. *Biochim. Biophys. Acta* **163**:20–29
- Gutknecht, J., Hastings, D.F., Bisson, M.A. 1978. Ion transport and turgor pressure regulation in giant algal cells. In: Membrane transport in biology, Vol. 3. Transport across multi-membrane systems. G. Giebisch, D.C. Tosteson and H.H. Ussing, editors, pp. 125–174. Springer Verlag, Berlin
- Heidecker, M., Wegner, L.H., Binder, K.-A., Zimmermann, U. 2003. Turgor pressure triggers characteristic changes in the electrical conductance of the tonoplast and the plasmalemma of the marine alga *Valonia utricularis*. *Plant Cell Environ.* in press
- Hieta, K., Kuga, S., Usuda, M. 1984. Electron staining of reducing ends evidences a parallel-chain structure in *Valonia* cellulose. *Biopolymers* **23**:1807–1810
- House, C.R. 1974. Water transport in cells and tissues. E. Arnold, editor. Monographs of the Physiological Society (Great Britain), London, No. 24
- Kaldenhoff, R., Eckert, M. 1999. Features and function of plant aquaporins. *J. Photochem. Photobiol.* **52**:1–6
- Kamiya, N. 1986. Cytoplasmic streaming in giant algal cells; A historical survey of experimental approaches. *Botanical Magazine Tokyo* **99**:441–467
- Kamiya, N., Tazawa, M. 1956. Studies on water permeability of a single plant cell by means of transcellular osmosis. *Protoplasma* **46**:394
- Katchalsky, A., Curran, P.F. 1965. Nonequilibrium thermodynamics in biophysics. Harvard Univ. Press, Cambridge
- Kedem, O., Katchalsky, A. 1958. Thermodynamic analysis of the permeability of biological membranes to non-electrolytes. *Biochim. Biophys. Acta* **27**:229–246
- Kedem, O., Katchalsky, A. 1961. A physical interpretation of the phenomenological coefficients of membrane permeability. *J. Gen. Physiol.* **45**:143–179

- Kedem, O., Katchalsky, A. 1963. Permeability of composite membranes: Part 1.-Electric current flow and flow of solute through membranes. *Trans. Faraday Soc.* **59**:1918–1930
- Kirk, K. 1997. Swelling-activated organic osmolyte channels. *J. Membrane Biol.* **158**:1–16
- Kirst, G.O. 1990. Salinity tolerance of eukaryotic marine algae. *Annu. Rev. Plant Physiol. Plant Mol. Biol.* **41**:21–53
- Koynova, R., Brankov, J., Tenchov, B. 1997. Modulation of lipid phase behavior by kosmotropic and chaotropic solutes. *Eur. Biophys. J.* **25**:261–274
- Läuchli, A., Kramer, D., Sluiter, E., Gullasch, J. 1976. Function of xylem parenchyma cells in ion transport through barley roots: localization of ions and of ATPases. *Echanges Ioniques Transmembranaires chez lex Vegetaux.* **258**:469–476
- Ling, G.N. 1987. On the large error introduced in the estimate of the density of membrane pores from permeability measurements when diffusion in “unstirred layer” within the cells is disregarded. *Physiol. Chem. Phys. Med. NMR* **19**:199–207
- McCully, M.E. 1970. The histological localization of the structural polysaccharides of seaweeds. *Ann. N. Y. Acad. Sci.* **175**:702–711
- Mussauer, H., Sukhorukov, V.L., Zimmermann, U. 2001. Trehalose improves survival of electrotransfected mammalian cells. *Cytometry* **45**:161–169
- Pate, J.S., Gunning, B.E.S. 1972. Transfer cells. *Annu. Rev. Plant Physiol.* **23**:173–196
- Philip, J.R. 1958. The osmotic cell, solute diffusibility, and the plant water economy. *Plant Physiol.* **33**:264–271
- Pohl, P., Saporov, S.M., Antonenko, Y.N. 1997. The effect of a transmembrane osmotic flux on the ion concentration distribution in the immediate membrane vicinity measured by microelectrodes. *Biophys. J.* **72**:1711–1718
- Richardson, I.W., Licko, V., Bartoli, E. 1973. The nature of passive flows through tightly folded membranes. The influence of microstructure. *J. Membrane Biol.* **11**:293–308
- Ryser, C., Wang, J., Mimietz, S., Zimmermann, U. 1999. Determination of the individual electrical and transport properties of the plasmalemma and the tonoplast of the giant marine alga *Ventricaria ventricosa* by means of the integrated perfusion/charge-pulse technique: evidence for a multifolded tonoplast. *J. Membrane Biol.* **168**:183–197
- Sauer, F.A. 1978. Nonequilibrium thermodynamics of isotope flow through membranes. In: Membrane transport in Biology. Vol. 3. Transport across Multi-Membrane Systems. G. Giebisch, D.C. Tosteson, H.H. Ussing, editors, pp. 141–168. Springer Verlag, Berlin
- Schneider, H., Zhu, J.J., Zimmermann, U. 1997. Xylem and cell turgor pressure probe measurements in intact roots of glyco-phytes: transpiration induces a change in the radial and cellular reflection coefficients. *Plant Cell Environ.* **20**:221–229
- Shepherd, V.A., Beilby, M.J. 1999. The effect of an extracellular mucilage on the response to osmotic shock in the charophyte alga *Lamprothamnium papulosum*. *J. Membrane Biol.* **170**:229–242
- Shepherd, V.A., Beilby, M.J., Heslop, D.J. 1999. Ecophysiology of the hypotonic response in the salt-tolerant charophyte alga *Lamprothamnium papulosum*. *Plant Cell Environ.* **22**:333–346
- Stein, W.D. 1967. The transport of molecules across cell membranes. Academic Press, New York
- Stento, N.A., Gerber Ryba, N., Kiegle, E.A., Bisson, M.A. 2000. Turgor regulation in the salt-tolerant alga *Chara longifolia*. *Plant Cell Environ.* **23**:629–637
- Sugiyama, J., Harada, H., Saiki, H. 1987. Crystalline morphology of *Valonia macrophysa* cellulose III₁ revealed by direct lattice imaging. *Int. J. Biol. Macromol.* **9**:122–130
- Sugiyama, J., Okano, T. 1990. Transformation of *Valonia* crystals by an alkaline hydrothermal treatment. *Macromolecules* **23**:3196–3198
- Tazawa, M., Kiyosawa, K. 1973. Analysis of transcellular water movement in *Nitella*: A new procedure to determine the inward and outward water permeabilities of membranes. *Protoplasma* **78**:349–364
- Tomos, A.D., Wyn Jones, R.G. 1988. Some transport properties of cells within tissues. In: Solute Transport in Plant Cells and Tissues. D.A. Baker, J.L. Hall editors, pp. 220–250. Longman, New York
- Toon, M.R., Solomon, A.K. 1996. Permeability and reflection coefficients of urea and small amides in the human red cell. *J. Membrane Biol.* **153**:137–146
- Tyerman, S.D., Steudle, E. 1984. Determination of solute permeability in *Chara* internodes by a turgor minimum method. Effects of external pH. *Plant Physiol.* **74**:464–468
- Verkman, A.S. 2000. Water permeability measurement in living cells and complex tissues. *J. Membrane Biol.* **173**:73–87
- Verkman, A.S., Dix, J.A. 1984. Effect of unstirred layers on binding and reaction kinetics at a membrane surface. *Anal. Biochem.* **142**:109–116
- Wang, J., Spiess, I., Ryser, C., Zimmermann, U. 1997. Separate determination of the electrical properties of the tonoplast and the plasmalemma of the giant-celled alga *Valonia utricularis*: vacuolar perfusion of turgescient cells with nystatin and other agents. *J. Membrane Biol.* **157**:311–321
- Zhang, Y.-H., Robinson, D.G. 1986. On the fixation of *Chlamydomonas reinhardtii*. *Ber. Deutsch. Bot. Ges.* **99**:179–188
- Zimmermann, U. 1978. Physics of turgor- and osmoregulation. *Ann. Rev. of Plant Physiol.* **29**:121–148
- Zimmermann, U. 1989. Water relations of plant cells: Pressure probe technique. *Methods Enzymol.* **174**:338–366
- Zimmermann, U., Hüsken, D. 1979. Theoretical and experimental exclusion of errors in the determination of the elasticity and water transport parameters of plant cells by the pressure probe technique. *Plant Physiol.* **64**:18–24
- Zimmermann, U., Råde, H., Steudle, E. 1969. Kontinuierliche Druckmessung in Pflanzenzellen. *Naturwissenschaften* **56**:634
- Zimmermann, U., Steudle, E. 1970. Determination of reflection coefficients of the membrane of the algae *Valonia utricularis*. *Z. Naturforsch. B* **25**:500–504
- Zimmermann, U., Steudle, E. 1974. The pressure-dependence of the hydraulic conductivity, the membrane resistance and membrane potential during turgor pressure regulation in *Valonia utricularis*. *J. Membrane Biol.* **16**:331–352
- Zimmermann, U., Steudle, E. 1978. Physical aspects of water relations of plant cells. *Adv. Bot. Res.* **6**:45–117
- Zimmermann, U., Steudle, E., Lelkes, P.I. 1976. Turgor pressure regulation in *Valonia utricularis*. *Plant Physiol.* **58**:608–613
- Zimmermann, U., Wagner, H.J., Heidecker, M., Mimietz, S., Schneider, H., Szimtenings, M., Haase, A., Mitlöhner, R., Kruck, W., Hoffmann, R., König, W. 2002. Implications of mucilage on pressure bomb measurements and water lifting in trees rooting in high-salinity water. *Trees* **16**:100–111
- Zimmermann, U., Zhu, J.J., Meinzer, F.C., Goldstein, G., Schneider, H., Zimmermann, G., Benkert, R., Thürmer, F., Melcher, P., Webb, D., Haase, A. 1994. High molecular weight organic compounds in the xylem sap of mangroves: Implications for long-distance water transport. *Bot. Acta* **107**:218–229